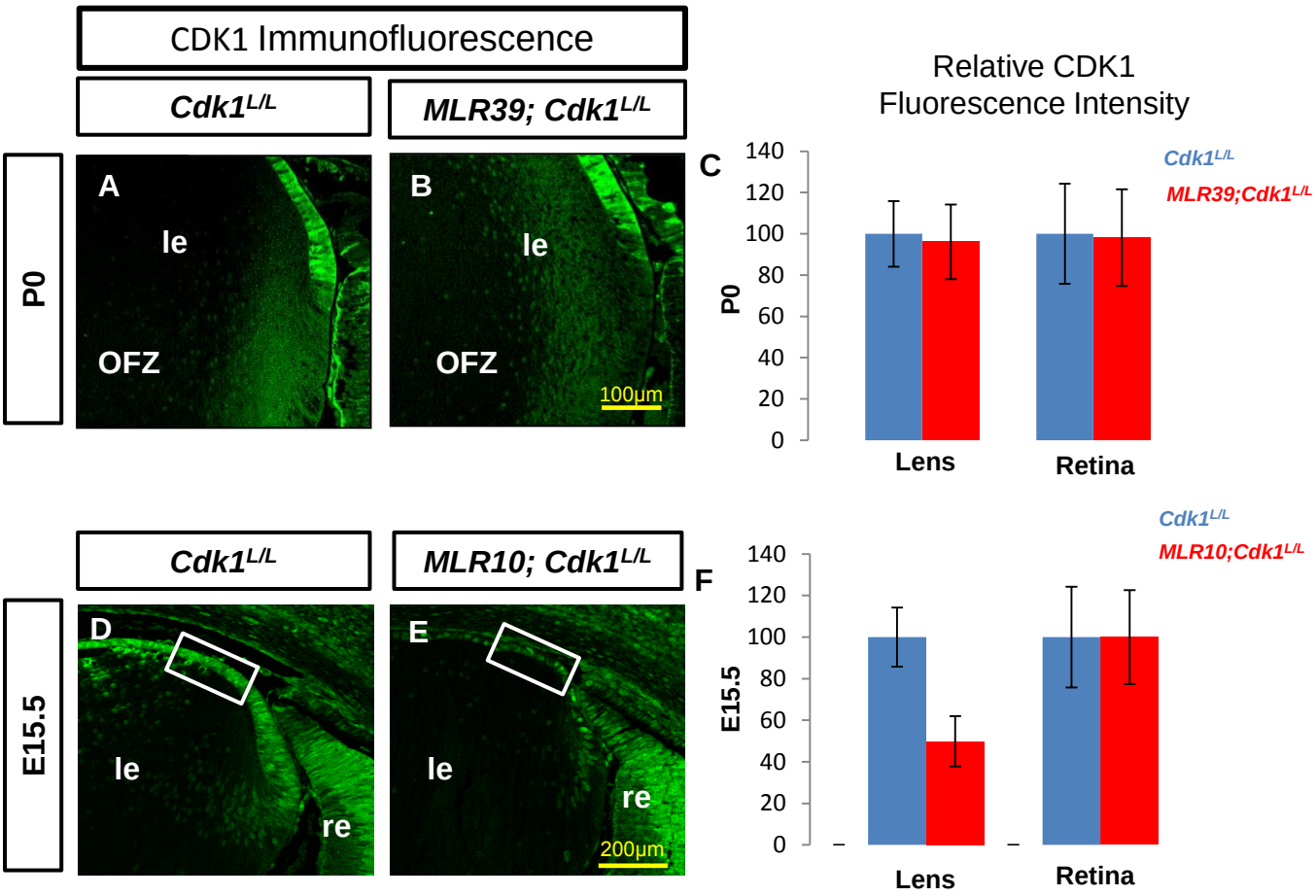

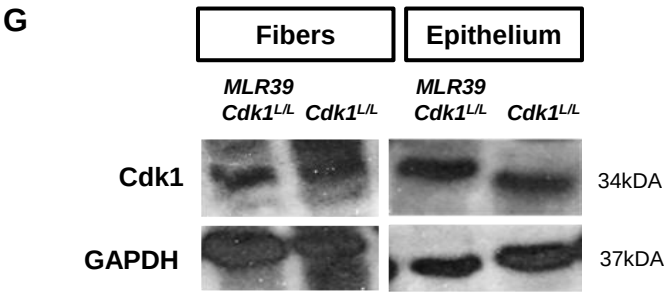

Supplemental Figure 1

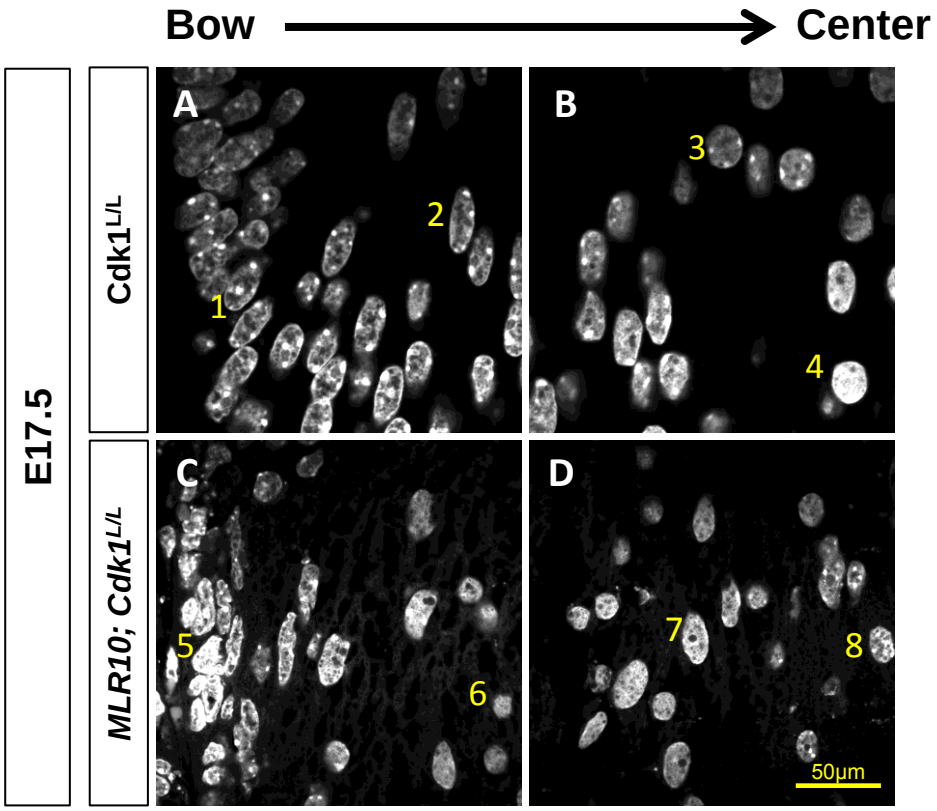

Supplemental Figure 2

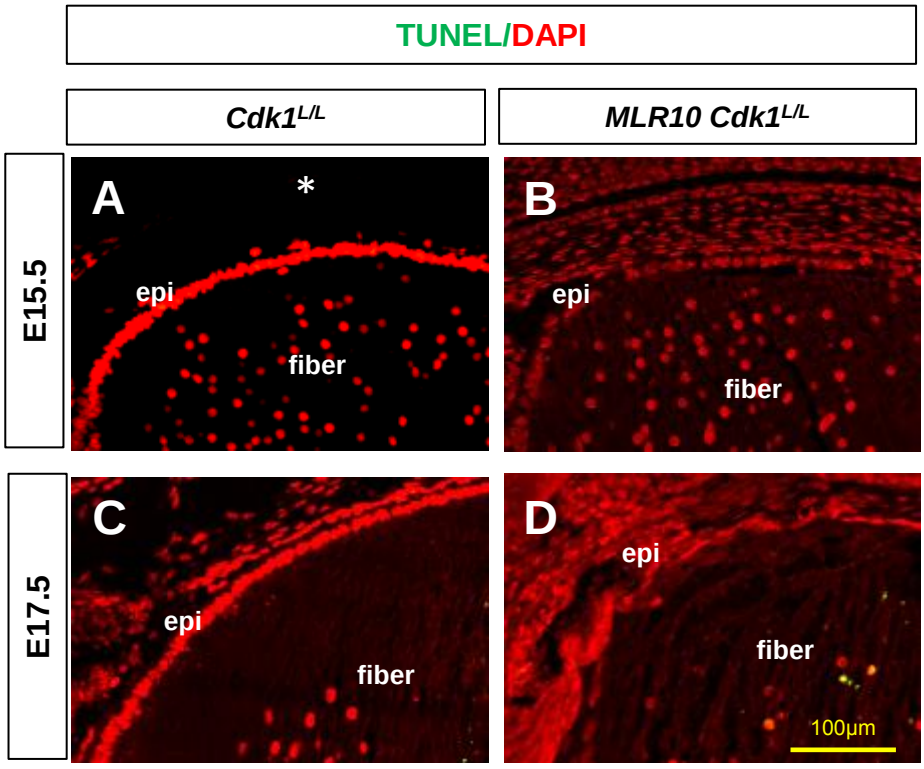

Supplemental Figure 3

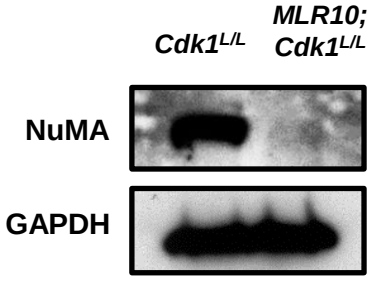

Supplemental Figure 4

Supplemental Figure Legends

Supp. Fig. 1

Cdk1$^{L/L}$ and *MLR39; Cdk1*$^{L/L}$ lenses were compared at P0 (birth) for CDK1 expression (A-C). CDK1 protein is evident in the lens epithelium and nuclei of fiber cells in *Cdk1*$^{L/L}$ lenses (A). The *MLR39* transgene did not reduce immunologically detectable CDK1 expression in the fiber cells of *MLR39; Cdk1*$^{L/L}$ mice (B, C). Western blot analysis supported the immunoflourescent data, as MLR39; Cdk1$^{L/L}$ lenses retained CDK1 protein in the fiber cell mass (G). *Cdk1*$^{L/L}$ and *MLR10; Cdk1*$^{L/L}$ lenses were compared at E15.5 for the expression of CDK1 (D-F). At E15.5 CDK1 was detected throughout the entire epithelium of *Cdk1*$^{L/L}$ lenses and in early differentiating fiber cell nuclei (D); whereas *MLR10; Cdk1*$^{L/L}$ lenses showed a mosaic pattern of CDK1 expression in the epithelium and almost no detectable CDK1 in the fiber cells (E). The fluorescent intensity for immunological detection of CDK1 was reduced 50% in *MLR10; Cdk*$^{L/L}$ lenses relative to the lenses of the of Cre negative controls lenses (F). However, the relative fluorescent intensity of CDK1 detection in the retina did not differ significantly between either the *MLR39; Cdk1*$^{L/L}$, and *Cdk1*$^{L/L}$ mice (C) or the *MLR10 Cdk1*$^{L/L}$ and *Cdk1*$^{L/L}$ mice (F). Relative fluorescent intensity of CDK1 in *MLR39; Cdk1*$^{L/L}$, and *MLR10; Cdk1*$^{L/L}$ lens and retina were measured by ImageJ software and normalized to the control lens and retina (C, F). Scale bars represent 100μm in A and B; 200μm in C-F.

Supp. Fig. 2

DAPI staining was implemented for nuclear structure analysis of *Cdk*$^{L/L}$ (A, B) and *MLR10; Cdk1*$^{L/L}$ (C, D) E17.5 lenses. Consistent nuclear structure changes occur moving inwardly from the lens bow (A) towards the lens center (B) in *Cdk1*$^{L/L}$ lenses. At the lens

bow, control lens nuclei are oval in shape and exhibit intense DAPI foci (A, nucleus 1 and 2). Moving towards the lens center, nuclei become spherical (B, nucleus 3), and contain an intense, even DAPI stain throughout the nucleus (B nucleus 4). *MLR10; Cdk1*$^{L/L}$ lenses do not exhibit consistent nuclear changes. Some nuclei near the bow region exhibit an intense DAPI stain throughout the nucleus, as if it were about to denucleate (C, nucleus 5), whereas some nuclei near the lens center are enlarged and oval shaped (D, nucleus 7 and 8).

Supp. Fig. 3 TUNEL analysis was implemented on E15.5 (A, B) and E17.5 (C, D) *Cdk1*$^{L/L}$ (A, C) and *MLR10; Cdk1*$^{L/L}$ (B, D) lenses to determine if increased apoptosis led to the reduction in epithelial cell number observed in *MLR10; Cdk1*$^{L/L}$ lenses. At E15.5 neither *Cdk1*$^{L/L}$ (A) or *MLR10; Cdk1*$^{L/L}$ (B) exhibited many TUNEL positive nuclei (green) in the epithelial cell layer, despite E15.5 *MLR10; Cdk1*$^{L/L}$ lenses already exhibiting noticeably fewer nuclei in the epithelial cell layer as indicated by the nuclear stain DAPI (red). Although the lens center of *Cdk1*$^{L/L}$ displayed numerous TUNEL positive foci by E17.5, the epithelial cell layer of both E17.5 *Cdk1*$^{L/L}$ (C) and *MLR10; Cdk1*$^{L/L}$ (D) lacked any detectable TUNEL positive signal. Sections were counterstained with DAPI (red) in A-D. Scale bar represents 100 μm in A-D.

Supp. Fig. 4

Western blot analysis using an antibody to NuMA revealed a reduction in total NuMA levels at E18.5 in *MLR10; Cdk1*$^{L/L}$ lenses (right lane) relative to the *Cdk1*$^{L/L}$ lenses (left lane). Anti-GAPDH was used as a loading control.